Steel and Composite Structures, *Vol. 24, No. 4 (2017) 383-390*
DOI: https://doi.org/10.12989/scs.2017.24.4.383

Behaviour of carbon fiber reinforced polymer strengthened tubular joints

P.S. Prashob *, A.P. Shashikala [a] and T.P. Somasundaran [b]

Department of Civil Engineering, National Institute of Technology Calicut, Calicut-673601, India

(*Received February 16, 2017, Revised March 31, 2017, Accepted April 02, 2017*)

Abstract. This paper highlights the experimental and numerical investigations performed on a tubular T-joint fabricated from circular hollow sections under axial compressive loads applied at the brace. Tests were performed on a reference joint and the joint wrapped with Carbon Fiber Reinforced Polymer (CFRP). The Nitowrap EP carbon fiber with Nitowrap 410 resin serve as a composite material is used for wrapping the T-joint. Schematic diagram of the fabricated tubular joint for the experimental test setup, along with the experimental and numerical results are presented. After performing these experiments, it has been demonstrated that the joint wrapped with CFRP has a better strength and lesser deflection than a reference joint. Finite element analysis carried out in Ansys reveals that the results were in good correlation with the experimental values.

Keywords: tubular joints; CFRP; Ansys; experimental investigation; finite element analysis

1. Introduction

Tubular members are widely used in the offshore scenario for the construction of offshore structures including jacket and jack-ups. The diameter to thickness ratio of these tubular members is larger compared to other structural applications. The current way of strengthening the tubular members in older platforms is to use external ring stiffeners, internal ring stiffeners and pass-through gusset plates. Thandavamoorthy (2004) studied the capacity of fatigue damage of tubular joints with internal ring stiffeners and stated that the predominant mode of deformation was bending of the chord member along its longitudinal axis.

Recently composite materials such as glass fiber reinforced polymers are being utilized for strengthening of tubular joints in the offshore industry. Carbon fiber composites find application in strengthening of columns and other parts of load bearing structures where improvement in shear strength is needed. Use of composites in the marine and offshore industry continues to increase drastically in the recent days.

Composites have slowly and steadily replaced the metals in new and existing structures because of its excellent properties. Carbon fiber composites are expensive for structural applications, but when high strength to weight ratio is required these composites are preferred. Carbon fiber composites are also corrosion resistant when used in the sea water environment. Tavakkolizadeh and Saadatmanesh (2003) found that by bonding CFRP laminates onto a steel-concrete composite girder, the load carrying capacity can be increased. Jones and Civjan (2003) had studied by wrapping CFRP on steel and concluded that the fatigue life of steel can be increased. Al-saidy *et al.* (2004) found that by using CFRP plates, the strength of damaged steel beams can be fully restored to its original strength.

Fawzia *et al.* (2007) studied normal and high modulus CFRP in retrofitting of hollow steel sections subjected to tensile force. The results showed that high modulus FRP is better than the normal modulus fiber. Seica and Packer (2007) carried out the rehabilitation of tubular steel structures using composite materials for the offshore industry and the reults show that the strengthening process was effective as all composite members exhibited improved structural performance. Zhao and Zhang (2007) studied the usage of FRP in strengthening and retrofitting of steel structures; FRP has become an alternate preference for retrofitting of civil structures. Teng and Hu (2007) compared the results of numerical and experimental work of compression tests conducted on a hollow tube wrapped with glass fiber sheets. Results show that FRP jacketing is a very promising technique for the retrofit and strengthening of circular hollow steel tubes. Haedir *et al*. (2009) compared normal hollow steel sections and CFRP strengthened steel sections subjected to pure bending.The tests reveal that the strength of composite is influenced by the amount of fiber reinforcement and the fiber orientation.

Ghafoori *et al*. (2012) studied theoretical and experimental work on notched steel beams, reinforced with prestressed and non- prestressed CFRP plates, subjected to cyclic loadings. Experimental results show that the fatigue life of a beam reinforced by the prestressed CFRP plate increases more than five times than that of a beam reinforced by non-prestressed CFRP plate. Parashar and Mertiny (2012) had done a review on adhesively bonded composite tubular joints and the results shows that an adhesive joint experiences uniform stress distribution, undamaged fibre architecture, and smooth surface contours.

*Corresponding author, Ph.D. Student,
E-mail: prashobpsb@gmail.com
[a] Professor
[b] Professor

http://www.techno-press.org/?journal=scs&subpage=6 ISSN: 1229-9367 (Print), 1598-6233 (Online)

Lesani *et al*. (2013a, b) did nonlinear static analysis of T-joints under axial brace compressive load, considering material and geometric nonlinearity with and without fiber reinforced polymer. Lesani *et al*. (2014) conducted studies on an unstrengthened and a glass fiber reinforced polymer (GFRP) wrapped joint. It was found that there was a significant improvement in the behavior of GFRP strengthened joint. Experimental and numerical results of unstrengthened and wrapped joints were in good correlation. No apparent failure or delamination was observed before the ultimate load.

Keykha (2016) used CFRP in strengthening steel columns subjected to eccentric loading. The results showed that the coverage length, the number of layers, and the location of CFRP composites were effective in increasing the ultimate load of the steel columns.

Although CFRP wrapping has been considered to be an efficient and suitable one for enhancing strength of tubular joints, there have been no previous attempts for its experimental verification, unlike GFRP known to us. In this research work, CFRP was wrapped onto the tubular T-joint for the strengthening purpose. The joint was fabricated from circular hollow sections to form a tubular joint, and CFRP was wrapped onto the joint. Finite element analysis was also performed to compare with the experimental work.

2. Experimental investigation

2.1 Details of tubular joint specimen

T-joints are fabricated using circular hollow tubes and tested under axial brace compressive loading. Fig. 1 shows the particulars of the tubular T-joint along with its dimensions and definitions. Table 1 lists the properties of the test specimen and the dimensionless parameters. TJ denotes an unreinforced T- joint while TJW represents the tubular joint with CFRP wrapping. Finite element analysis was carried out to fix the appropriate geometric dimensions and to eliminate the chord end effects.

The chord diameter was 273.1 mm whereas the brace diameter was 114.3 mm. The tubular joint was thus designed with a chord length of 1740 mm between the supports while the brace length was fixed to 583.45 mm to satisfy the chord slenderness ratio. The T-joint was fabricated using seamless hot finished carbon steel pipe following American Society for Testing and Materials (ASTM) standards, ASTM A106/A106M (2016) with a minimum yield strength of 240 MPa and ultimate tensile strength of 415 MPa. Gas cutting was used to cut the profile of the brace member. The initial setup of joining of chord and brace using tack welding is shown in Fig. 2.

As per guidelines from Shielded Metal Arc Welding SMAW (2013), the brace was connected to the chord member to form a tubular joint. As per the standard, the electrode used for welding is E7018. E indicates it is an electrode, 70 indicates how active this electrode is when welded, 1 shows the welding positions that can be used such as flat, horizontal, vertical and overhead and 8 indicates the coating (i.e., Low Hydrogen Iron Powder). The electrode has got an yield and ultimate strength of 393 MPa and 482 MPa respectively.

Two, 20 mm thick steel plates are welded to the chord ends and one 20 mm thick steel plate, to the brace end of the T-joint. The chord end was fitted into the compression testing machine with the help of the supports to assist the specimen installation, and the axial load was then applied to the brace end. Full penetration welds were used for the brace-chord intersection and pipe to end plates for preventing failure, while fillet welds were used to connect stiffener plates. Welds were subjected to non-destructive testing using a dye test to check the quality of weld such that no failure occurs at the weld region while loading.

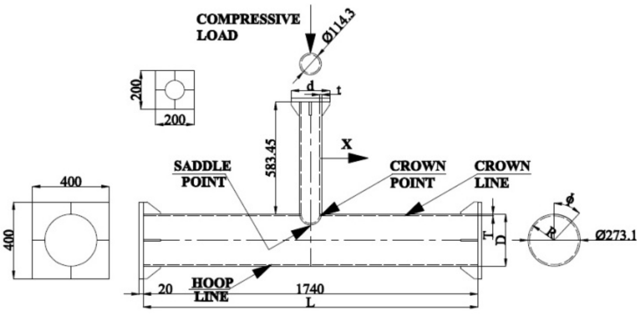

Fig. 1 Details of tubular joint

Fig. 2 Tube connection and tack welding

Table 1 Tubular joint property

	D (mm)	d (mm)	T (mm)	t (mm)	L (mm)	θ	α	β	γ	τ
Specimen TJ/TJW*	273.1	114.3	9.27	8.56	1740	90	12.72	0.42	14.73	0.92

* TJ: Tubular Joint; TJW: Wrapped Tubular Joint

Table 2 Tensile test coupon properties

	Width (mm)	Thickness (mm)	Yield load (kN)	Ultimate load (kN)	Yield stress (MPa)	Ultimate stress (MPa)
Brace	26.4	7.8	93.35	107.7	453.33	523.01
Chord	40.2	10.2	185.24	214.2	451.75	522.38

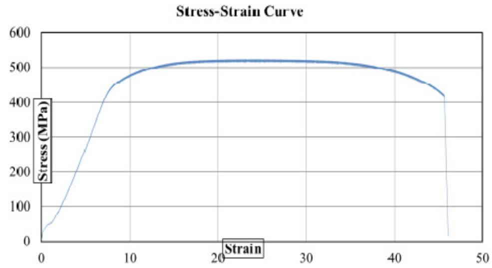

Fig. 3 Details of tensile test

2.2 Tension test

Strain-controlled tensile testing of the specimen was done using computer controlled electro-hydraulic servo universal testing machine model WAW-1000E to determine the mechanical properties of the brace and the chord member. In this test, tensile coupons from the same material following ASTM standards (ASTM E8/E8M 2016) are subjected to a gradual pull at a strain rate between 0.05 and 0.5 mm/min. Testing of the full section of larger diameter tube cannot be performed, so longitudinal tension test specimens taken from the hollow tube served the purpose. For seamless pipes, the section can be cut from any curved area as it is free from the weld, and then the specimen was flattened without the application of heat. The extensometer gauge length was set to 50 mm. Table 2 presents the results of the tensile test and Fig. 3 shows the stress-strain curve along with the test coupons.

2.3 Properties of carbon fiber

The composite material consists of two parts such as fiber and the matrix (resin/ saturant). These fibers, mixed with matrix forms a composite material which is used to strengthen the tubular structure. The fiber Nitowrap EP carbon fiber in which its orientation is unidirectional, and the matrix used here is of Nitowrap 410 supplied by Fosroc Constructive Solutions. The matrix, used here, consists of two parts which are mixed in the right proportion as per the manual to achieve the desired results, which serves as a binding medium for the fibers. It can be applied to any shape or contour due to its flexibility and can be effectively used in space-constrained areas. It is quite economical, and thus, easy to install and time and labor saving. Tables 3 and 4 show the details of the fiber and resin properties.

To determine the orthotropic properties of the composite material, tensile tests in the longitudinal and transverse directions need to be performed. By preparing the specimens as per ASTM standards ASTM D 3039/D3039M (2005), the tensile modulus in the three directions is obtained. By measuring the lateral strain to the longitudinal strain, Poisons ratio is obtained in the in- plane direction. For obtaining the shear modulus, a tensile test is performed on the composite material by preparing the specimen as per ASTM standards ASTM D3518/D3518M (2016) or by the V-Notched method following ASTM standards ASTM D5379/D5379M (2016).

2.4 CFRP wrapping

The tubular joint surface where carbon fiber wrapping is to be done is cleaned from surface impurities. The region where CFRP application is to be done, the surfaces is slightly abraded such that the matrix sticks to the tubular joint properly. After welding of the brace chord intersection, the profile was smoothened with a grinder to achieve a

Table 3 Properties of carbon fiber

Fiber	Tensile modulus (GPa)	Fiber thickness (mm)	Weight of fiber (g/m^2)
Nitowrap EP	285	0.11	200

Table 4 Properties of primer and saturant

	Density (g/cc)	Pot life (mm)	Full care (days)
Nitowrap 30	1.14	25	7
Nitowrap 410	1.25-1.26	120	5

Fig. 4 Nitowrap 30 primer applied on the joint

smoother profile. Water paper was then used to abrade the surface so that it was free from dust and with the help of a vacuum cleaner, all the dust was then removed to make it dust free. The acetone solution was used to clean the surface of the tubular structure.

After cleaning the joint surface with acetone, Nitowrap 30 primer was applied to the area, where carbon fiber was to be wrapped, while the rest of the area was painted with oil primer to prevent the part from rusting. Fig. 4 shows the primer application on the tubular joint. Mixing of Nitowrap 30 primer was as per the manual and application of the primer was done and it was allowed to dry for about 24 hours before applying the saturant. The Nitowrap 410 saturant which consists of a base and hardener was mixed for about 3 minutes as per the manual to form a uniform color of pale yellow to amber. Later, the saturant was applied over the primer, and the unidirectional carbon fiber sheets already cut according to the template which has been prepared earlier, was wrapped to the saturant with the help of gloves, followed by a roller.

A template was cut from the fiber sheets to accommodate the obstruction of the brace member. For each subsequent layers, necessary adjustment was made to compensate for the template length as this got increased around the circumference of the chord member. The carbon fiber sheets available with the following width of 500 mm satisfied 10√DT. The pot life of the saturant is limited to 2 hours, so, the wrapping of CFRP is finished within this time.

Hand lay-up technique was employed to wrap the fiber sheets, the saturant was applied to the tubular joint uniformly using a putty knife, and the laying of fiber sheets was done with utmost care to prevent entrapped air as this may cause bulging at certain locations. At the intersection areas, a roller brush was used to place the fiber sheets in position. The tubular joint was kept in a vertical position, so that, applying of saturant and placing of carbon fiber sheets could be done at ease.

The minimum cure time for the saturant and primer are 5 and 7 days respectively. Before testing, the tubular joint was cured for 28 days. Fig. 5 shows the CFRP reinforcement directions. The fiber was having a thickness of 0.11 mm, while the thickness of each ply was measured and found to be 0.5 mm. The total thickness around the chord member was nearly 5 mm and at the brace chord intersection, it experiences a cumulative thickness of both the brace and the chord member. CFRP was wrapped onto tubular joints as per the orientation which is illustrated in Table 5. Fig. 6 shows the wrapping of CFRP on the tubular joint by hand layup technique.

2.5 Instrumentation

The test arrangement is shown in Fig. 7, in which the tubular joints were subjected to an axial compressive load. The tubular joint was placed under a compression testing machine in which both ends of the chord are fixed to the supports of the compression testing machine using end plates of thickness 20 mm. The compression testing machine was fixed to the strong concrete floor using high

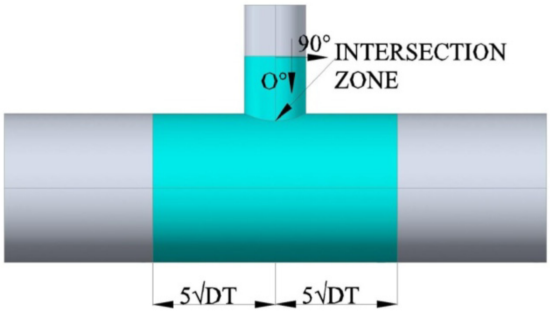

Fig. 5 CFRP reinforcement direction

Fig. 6 Wrapping of CFRP on Tubular joint

Table 5 CFRP Orientation

	Orientation scheme	Ply thickness (mm)	Total ply thickness (mm)
Brace	[0/90/0/90/0/0]	0.5	3
Chord	[0/45/-45/0/-45/45/0]	0.5	3.5
Brace-chord intersection	[0/0/90/45/0/-45/90/0/0/-45/0/45/0]	0.5	6.5

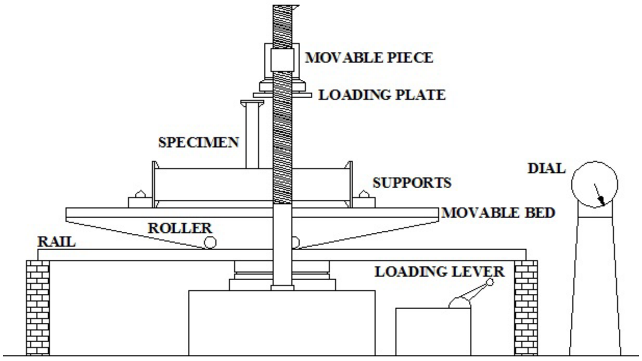

Fig. 7 Specimen on compression and bending testing machine

strength bolts. The axially compressive force was then applied to the brace of the T-joint by the compression testing machine, with a maximum capacity of 300 tons. Initially, loading was applied to the T-joint to check the operation of the strain gauges and linear variable differential transformer (LVDT) and it was subsequently unloaded to check that the instrumentation readings returned to zero.

Force control loading was used to perform the axial compressive load on the brace end. The hydraulic pump was operated to move the loading plate slowly till it touched the brace plate. An initial load was applied to the T-joint for better contact; this reduced the gap between the T-joint and the loading plate. The readings of LVDTs were recorded by the displacement reader and strain gauges reading were noted at each loading intervals, using a 20 channel data acquisition system. For the reference tubular joint TJ, a strain gauge was installed on the crown and saddle points, and for the wrapped tubular joint TJW the strain gauge was fixed on the same locations of the reference joint but under the first layer of CFRP. Fig. 8 shows the specimen arrangement of reference and wrapped joint on the testing machine. Fig. 9 shows the LVDT and strain gauge arrangement.

3. Numerical investigation using Ansys

Shell elements have the ability for bending, so they are often used to model the tubular joint. Representation of weld is difficult with the shell model, so it is ignored in the present study. Only the mid-surface can be modeled using shell elements for the structural analysis of tubular joint. In this analysis, Shell281 is used with eight nodes, and six degrees of freedom allotted to each node: translations and rotations in the three axes Ansys inc. (2007).

4. Results and discussions

The discussion on experimental results carried out on the tubular joint are divided into different sections. For each loading, the vertical displacement and ovalization were measured, failure modes of two different specimens were also carried out. Maximum stresses experienced by the specimens were also noted. A dimensionless parameter

Fig. 8 Specimen arrangement on compression and bending testing machine

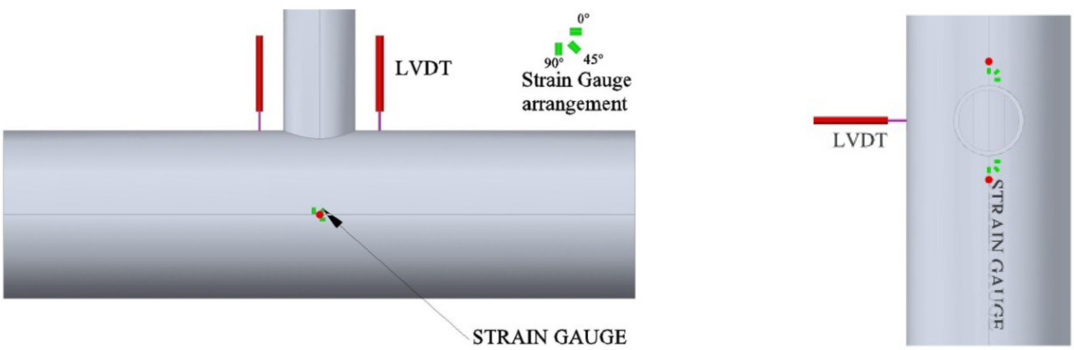

Fig. 9 Instrumentation arrangement on specimen (Front view and top view)

called effective chord shell width equal to √DT is defined to monitor the locations on chord surface, for the longitudinal direction, the distance is measured from the tubular center towards the chord end (X) Lesani *et al*. (2014). The crown point is located at X/√DT = 1.14, and the saddle point is located at RΦ/√DT = 1.18 for the T-joint. RΦ is the distance measured from the plug center towards the chord quadrants on the curved surface in the hoop direction. Due to the symmetrical behavior of the structure, half of the chord member surface in the hoop direction was investigated.

4.1 Load-displacement

The load versus vertical displacement of the tubular joint is plotted for the two cases, and the comparison is made between the numerical and experimental values. Vertically placed LVDTs were used to measure the vertical displacements of the tubular joint. Crown points experienced the maximum displacement and when the ends of chord are reached the vertical displacement got reduced. Numerical and experimental investigations are in a good correlation. It reveals that the tubular joint, wrapped with CFRP experienced less deflection, compared to the standard tubular joint. 56% reduction in deflection was observed for the tubular joint with CFRP wrapping. Fig. 10 shows the load-displacement diagram for the tubular joint. Fig. 11 illustrates the comparison of the chord surface displacement of the reference joint and the wrapped joint.

4.2 Load-ovalization

Ovalization is the horizontal deflection in the cross section of the brace chord intersection, i.e., on the hoop line. When a compressive load is applied to the tubular joint, there is a local deformation at the chord surface. Horizontally placed LVDTs were used to measure the ovalization of the tubular joint. 67% reduction in ovalization was observed for the tubular joint with CFRP wrapping.. Maximum ovalization displacement for the tubular joint occurs at RΦ/√DT = 4.4. This location is where the maximum bulging occurs when the axial compressive load was applied. Fig. 12 shows the load-ovalization displacement diagram for the tubular joint. Fig. 13 illustrates the comparison of the ovalization of the reference joint and the wrapped joint.

4.3 Stress-strain investigations

Strain gauges were located on the tubular joints on the crown and hoop line as indicated in the instrumentation diagram. For the wrapped joint, the strain gauge was installed below the first layer of CFRP at the same locations of the reference joint so that comparisons can be made. The maximum stress for the reference joint was matching with the yield stress values of tensile test conducted on the same material. By wrapping CFRP onto the tubular joint the stress values got reduced. The results of experimental investigations and finite element analysis compared by

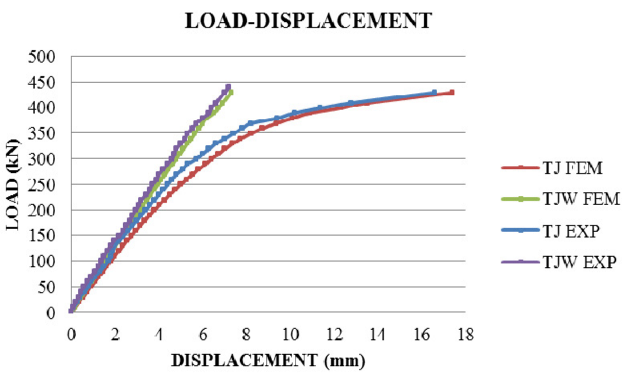

Fig. 10 Load - displacement diagram
(TJ FEM - Numerical Investigation on Reference Joint,
TJW FEM - Numerical Investigation on Wrapped Joint,
TJ EXP - Experimental Investigation on Reference Joint,
TJW EXP - Experimental Investigation on Wrapped Joint)

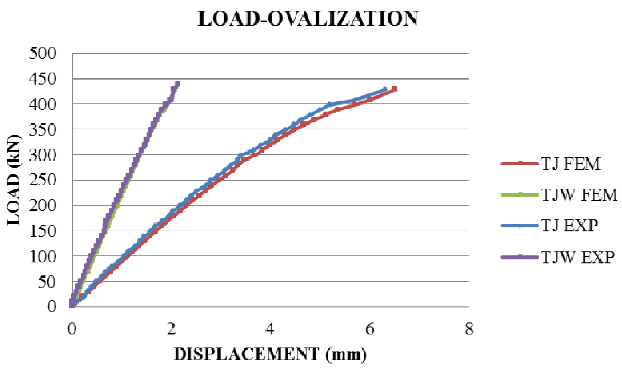

Fig. 12 Load - ovalization diagram
(TJ FEM - Numerical Investigation on Reference Joint,
TJW FEM - Numerical Investigation on Wrapped Joint,
TJ EXP - Experimental Investigation on Reference Joint,
TJW EXP - Experimental Investigation on Wrapped Joint)

Fig. 11 Chord surface deflection

Fig. 13 Ovalization

Table 6 Comparison of stress strain values

Detail	Load (kN)	Maximum stress (MPa)	Maximum strain
TJ FEM	120.00	446.27	0.00210
TJ EXPMT	119.57	444.65	0.00212
TJW FEM	120.00	355.68	0.00170
TJW EXPMT	119.57	354.40	0.00160

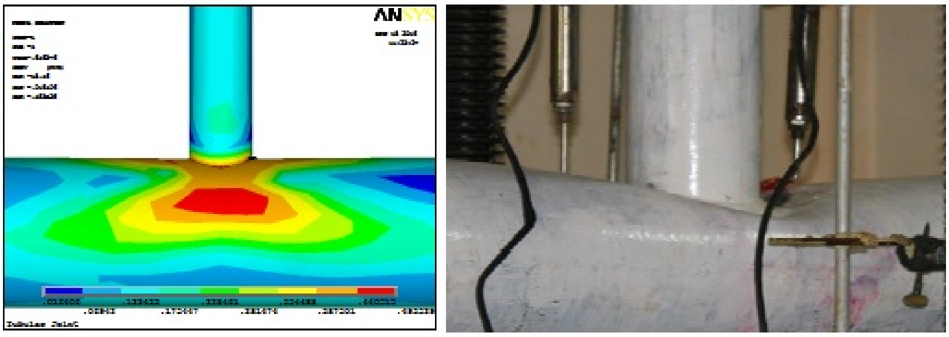

Fig. 14 Numerical and experimental investigations of TJ showing punching shear stress

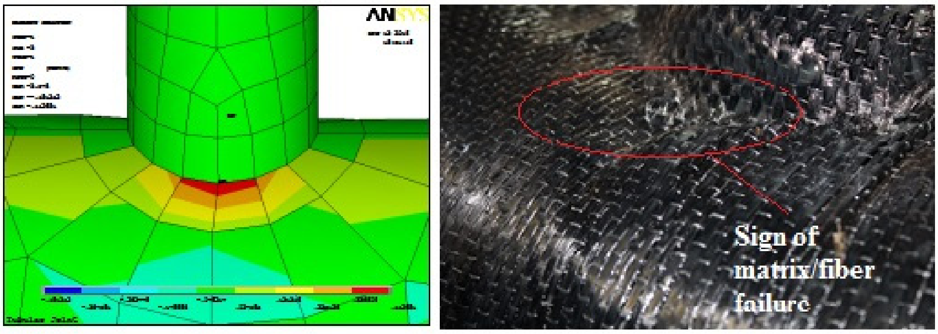

Fig. 15 Numerical and experimental investigations of TJW showing a sign of matrix/fiber failure

evaluating the strain gauge reading with the nodal values of numerical investigation are shown in Table 6.

4.4 Types of failure

For the ultimate load, the reference joint failed by punching shear, while CFRP prevented the wrapped joint against punching shear. For the same loading CFRP wrapped joint experienced only a sign of matrix fiber failure at the brace chord intersection. For the wrapped joint, at a load of 200 kN, initial cracking sound occurred which was for the matrix failure, and at a load of 330 kN, repeated cracking sound was observed which was for fiber matrix breakage. At 400 kN, the crack sound was more, but no delamination occurred. This suggests that the CFRP has an acceptable bond with the steel tubular joint. After reaching the ultimate load, the wrapped specimen was taken out from the compression testing machine, and CFRP was removed from the wrapped joint to visualize how much ovalization and vertical displacement occurred in the wrapped tubular joint. It was found that compared to the reference joint, it experienced only less deformation, which showed the contribution of FRP in taking the load. A thorough inspection was done for both the tubular joints after loading, and there was no defect found in the welding. Figs. 14 and 15 show the numerical and experimental counterpart of the tubular joints subjected to punching shear stress and matrix/fiber failure respectively.

5. Conclusions

The experimental and numerical investigations carried out revealed the following conclusions:

By wrapping CFRP in tubular joint, 56% reduction in chord surface deflection and 67% reduction in ovalization was observed. The stresses get reduced by 20% for the CFRP joint when compared with the reference joint. The initial matrix failure occured in the CFRP wrapped tubular joint at 55% of the ultimate load. The reinforcement length covered the area where displacement and ovalization occur. No sign of delamination or debonding happened in the wrapped area. Numerical and experimental investigations showed a good relationship for both the reference and the wrapped joints. A sign of matrix/fiber failure occurred at the intersection of the wrapped joint which show that the composite escort the steel under loading. Feasibility in retrofitting of existing joints in offshore structures can be performed.

Acknowledgments

The authors are thankful to the National Institute of Technology Calicut (NITC) for the financial support in procuring and fabrication of test specimens and providing the basic experimental setup. The authors also thank, Fosroc Constructive Solutions, Bangalore for providing Nitowrap Chemicals.

References

Aguilera, J. and Fam, A. (2013), “Retrofitting tubular steel T-joints subjected to axial compression in chord and brace members using bonded FRP plates or through-wall steel bolts”, *Eng. Struct.*, **48**, 602-610.

Al-saidy, A.H., Klaiber, F.W. and Wipf, T.J. (2004), “Repair of steel composite beams with carbon fiber-reinforced polymer plates”, *J. Compos. Constr.*, **8**(2), 163-172.

Ansys inc. (2009), http://www.ansys.com

ASTM A106/A106M (2016), Standard Specification for Seamless Carbon Steel Pipe for High-Temperature Service; American Society for Testing and Materials, PA, USA.

ASTM D3039/D3039M (2005), Standard Test Method for Tensile Properties of Polymer Matrix Composite Materials; American Society for Testing and Materials, PA, USA.

ASTM D3518/D3518M (2016), Standard Test Method for In-Plane Shear Response of Polymer Matrix Composite Materials by Tensile Test of a ± 45° Laminate; American Society for Testing and Materials, PA, USA.

ASTM D5379/D5379M (2016), Standard Test Method for Shear Properties of Composite Materials by the V-Notched ASTM D5379/D5379M; American Society for Testing and Materials, PA, USA.

ASTM E8/E8M (2016), Standard Test Methods for Tension Testing of Metallic Materials; American Society for Testing and Materials, PA, USA.

Fawzia, S., Al-Mahaidi, R., Zhao, X.L. and Rizkalla, S. (2007), “Strengthening of circular hollow steel tubular sections using high modulus CFRP sheets”, *Constr. Build. Mater.*, **21**(4), 839-845.

Ghafoori, E., Schumacher, A. and Motavalli, M. (2012), “Fatigue behavior of notched steel beams reinforced with bonded CFRP plates: Determination of prestressing level for crack arrest”, *Eng. Struct.*, **45**, 270-283.

Haedir, J., Bambach, M.R., Zhao, X.L. and Grzebieta, R.H. (2009), “Strength of circular hollow sections (CHS) tubular beams externally reinforced by carbon FRP sheets in pure bending”, *Thin-Wall. Struct.*, **47**(10), 1136-1147.

Jones, S.C. and Civjan, S.A. (2003), “Application of fiber reinforced polymer overlays to extend steel fatigue life”, *J. Compos. Constr.*, **7**(4), 331-338.

Keykha, A.H. (2016), “CFRP strengthening of steel columns subjected to eccentric compression loading”, *Steel Compos. Struct., Int. J.*, **23**(1), 87-94.

Lesani, M., Bahaari, M.R. and Shokrieh, M.M. (2013a), “Detail investigation on un-stiffened T/Y tubular joints behavior under axial compressive loads”, *J. Constr. Steel Res.*, **80**, 91-99.

Lesani, M., Bahaari, M.R. and Shokrieh, M.M. (2013b), “Numerical investigation of FRP-strengthened tubular T-joints under axial compressive loads”, *Compos. Struct.*, **100**, 71-78.

Lesani, M., Bahaari, M.R. and Shokrieh, M.M. (2014), “Experimental investigation of FRP-strengthened tubular T-joints under axial compressive loads”, *Constr. Build. Mater.*, **53**, 243-252.

Parashar, A. and Mertiny, P. (2012), “Adhesively bonded composite tubular joints: Review”, *Int. J. Adhesion Adhesives*, **38**, 58-68.

Seica, M.V. and Packer, J.A. (2007), “FRP materials for the rehabilitation of tubular steel structures, for underwater applications”, *Compos. Struct.*, **80**(3), 440-450.

SMAW (2013), Guidelines for Shielded Metal Arc Welding; Appleton, WI 54914, USA.

Tavakkolizadeh, M. and Saadatmanesh, H. (2003), “Fatigue strength of steel girders strengthened with carbon fiber reinforced polymer patch”, *J. Struct. Eng.*, **129**(2), 186-196.

Teng, J.G. and Hu, Y.M. (2007), “Behaviour of FRP-jacketed circular steel tubes and cylindrical shells under axial compression”, *Constr. Build. Mater.*, **21**(4), 827-838.

Thandavamoorthy, T.S. (2004), “Reserve capacity of fatigue damaged internally ring stiffened tubular joints”, *Steel Compos. Struct., Int. J.*, **4**(2), 149-167.

Zhao, X.L. and Zhang, L. (2011), “State-of-the-art review on FRP strengthened steel structures”, *Eng. Struct.*, **29**(8), 1808-1823.

BU